tree-ring index and isotopes measured on the GISP2 ice core [J. W. C. White, D. Gorodetzky, E. R. Cook, L. K. Barlow, in *Climate Variations and Forcing Mechanisms of the Last 2000 Years*, P. D. Jones, R. S. Bradley, J. Jouzel, Eds. (Springer-Verlag, Berlin, 1996), vol. 41, pp. 193–212].
15. C. Torrence and G. P. Compo, *Bull. Am. Meteorol. Soc.* **79**, 61 (1998). For a review, see P. Kumar and E. Foufoula-Georgiou, *Rev. Geophys.* **35**, 385 (1997).
16. S. Baliunas, P. Frick, D. Sokoloff, W. Soon, *Geophys. Res. Lett.* **24**, 1351 (1997).
17. T. F. Stocker and L. A. Mysak, *Clim. Change* **20**, 227 (1992). T. F. Stocker, *NATO ASI* **I44**, 379 (1996).
18. N. Mahasenan, R. G. Watts, H. Dowlatabadi, *Geophys. Res. Lett.* **24**, 563 (1997); M. E. Schlesinger and N. Ramankutty, *Nature* **367**, 723 (1994).
19. M. E. Mann, R. S. Bradley, M. K. Hughes, *Nature* **392**, 779 (1998).
20. Current theoretical and numerical models are reviewed in M. Latif, *J. Clim.* **11**, 602 (1998).
21. T. Delworth, S. Manabe, R. J. Stouffer, *ibid.* **6**, 1993 (1993).
22. Data not shown.
23. S. M. Griffies and K. Bryan, *Science* **275**, 181 (1997).
24. C.A. was supported by the National Swiss Science Foundation (SPPU, CLEAR2). Special thanks to ECMWF; Swiss Met Office (SMA); D. Lüthi, J. W. Hurrell, P. D. Jones, and E. R. Cook for providing their data; and B. Stauffer, J. Schwander, and S. Sommer for fruitful conversations.

29 June 1998; accepted 9 September 1998

Two-Dimensional Magnetic Particles

C. Stamm, F. Marty, A. Vaterlaus, V. Weich, S. Egger, U. Maier, U. Ramsperger, H. Fuhrmann, D. Pescia*

Single two-dimensional (2D) atomically thick magnetic particles of cobalt and iron with variable size and shape were fabricated by combining a mask technique with standard molecular beam epitaxy. Reduction of the lateral size of in-plane magnetized 2D cobalt films down to about 100 nanometers did not essentially modify their magnetic properties; although the separation of boundaries decreased greatly, neither domain penetrated the particle, nor was any sizable shape anisotropy observed. The mutual interaction of 2D cobalt particles was negligible, and the magnetic state of a single particle could be switched without modifying the state of the neighbors. Perpendicularly magnetized iron particles did not exhibit such responses. These results suggest that only a few atoms forming a 2D in-plane magnetized dot may provide a stable elementary bit for nanorecording.

Consider the effects of reducing the lateral dimensions of a magnetic film so that a flat particle is produced. At least two questions arise. First, as the boundaries are coming closer, their demagnetizing action—which is negligibly small, for example, at in-plane magnetized extended films (*1–3*)—is expected to increase. As a result, it might become energetically favorable for domains to penetrate the particle when its lateral size is reduced (*4*). Simultaneously, the shape of the particle (*5–8*) might compete with the magnetocrystalline anisotropy (*9*) to determine the direction of the magnetization M. The second question arises in connection with an ensemble of such particles: The dipolar energy responsible for possible demagnetizing effects within one single particle produces a long-range interaction between the particles. Thus, it might become impossible to change the magnetic state of a particle without affecting the state of the neighbors. As the geometry of the particles and their mutual interaction lead to the complicated magnetic behavior observed in mesoscopic magnets (*4–6, 10–14*), the answers to these two questions are of fundamental importance for possible applications such as magnetic recording.

We addressed these two questions in the limit of atomically thin films of Co on Cu(100). Co/Cu(100) seems to represent a model system for in-plane magnetized ultrathin films (*3, 9, 15–19*) and should provide a suitable reference for starting the patterning operation. The ultraflat particles are produced by molecular beam epitaxy (MBE) (*16, 20*) under ultrahigh-vacuum conditions (10^{-11}-mbar range). Lateral patterning is achieved in situ during MBE by placing a diaphragm between the MBE source and the substrate. This diaphragm consists of a 1-μm-thick foil with microholes that had been etched with a commercial focused ion beam (FIB) system. The magnetization was measured in situ and resolved spatially with two techniques: scanning Kerr microscopy (SKEM, lateral resolution of 1 μm) (*16*) and scanning electron microscopy with polarization analysis (SEMPA, lateral resolution of ~10 nm) (*3, 18, 21, 22*). Sample growth and measurements were performed at room temperature. The thickness of the microstructures was determined by calibrating the evaporation rate with Auger spectroscopy and scanning tunneling microscopy (STM) (*16, 20*) performed on continuous films. On selected microstructures, we cross-checked the thickness by STM. In addition, we used SEMPA to measure the electron spin polarization P as a function of thickness. This allowed an additional thickness calibration that was particularly important for the smallest structures, which turned out to be thinner than expected from the evaporation rate. The sharpness of the boundary of the microstructures, determined by STM, was ~100 nm.

The spatially resolved remanent state magnetization M (zero applied magnetic field H) of ultraflat particles (thickness δ typically in the range 2 AL < δ < 10 AL, where AL = atomic layer) is shown in Fig. 1 for lateral sizes varying from ~1 mm to ~100 nm. All of the particles are ferromagnetic starting from $\delta \approx 2$ AL; the easy (energetically most favored) M axis is in-plane and along the same crystallographic direction for all of the particles, irrespective of their size and shape. Each particle has a roughly square hysteresis loop (Fig. 1D) with a nearly fully magnetized remanent state, and M is homogeneously distributed; no magnetic domains penetrate the particles even when their size is varied over many decades. A minimum magnetic field H_{rev} is required to switch M of the particles in the opposite direction (see Fig. 1D and the transition from Fig. 1F to Fig. 1G). We studied the magnetic state close to H_{rev}—that is, close to the state of instability toward reversing M—by applying a reverse magnetic field $H_{rev} - \Delta H_{rev}$ (the field was successively switched off to perform the SEMPA imaging). We observed a single-domain state up to reverse applied fields very close to H_{rev} (the smallest values of $\Delta H_{rev}/H_{rev}$ achieved in our study were 0.005). Thus, the microstructures switched from one homogeneous state to the reverse state. With current imaging methods, we are not yet able to determine how this switching (that is, the time evolution of M at H_{rev}) proceeded.

An exception to the single-domain rule is the millimeter-sized Co film seen in Fig. 1B, where millimeter-sized domains are produced in the vicinity of H_{rev}. However, over such large scales, the Co film is bound to meet with the major structural defects provided by the Cu surface and to develop enough magnetostatic energy E_m to create domains and pin their walls. These defects are most likely determining the value of H_{rev} in microstructures as well: H_{rev} increased with thickness (*15*) but did not show any systematic variation with size and shape.

C. Stamm, F. Marty, A. Vaterlaus, V. Weich, S. Egger, U. Maier, D. Pescia, Laboratorium für Festkörperphysik, Eidgenössische Technische Hochschule (ETH) Zürich, CH-8093 Zürich, Switzerland. U. Ramsperger, National Research Institute for Metals, 1-2-1 Sengen, Tsukuba, Ibaraki 305, Japan. H. Fuhrmann, Institut für Teilchenphysik, ETH Zürich, CH-8093 Zürich, Switzerland.

*To whom correspondence should be addressed.

To explore the influence of the particle shape on its magnetic state, we have investigated the spatial distribution of M in ultraflat magnetic stripes, which are the 2D counterpart of 3D magnetic needles. The magnetostatic energy stored in needles magnetized along the axis is much smaller than that of needles magnetized perpendicular to the axis; this shape anisotropy forces the 3D needles to be magnetized along the axis. In contrast, no such shape anisotropy is observed in 2D stripes. Inspection of an array of stripes 50 μm long and 1 μm wide (in-plane aspect ratio $R = 50$) oriented at a variable angle α with respect to the easy M axis (Fig. 2A) showed that M is uniform within each stripe and points in the same direction for all α. A detailed analysis of the spin polarization of stripes with $R = 80$ (Fig. 2B) confirmed that varying α does not produce any measurable deviation from the vertical orientation. For very thin stripes with $R = 80$, we have calculated, using the methods of (*23*), that the shape anisotropy field favoring the stripe axis is (in oersteds) approximately $\delta \cdot 7 \cdot \sin^2 \alpha$. This is comparable to H_{rev} and about one order of magnitude smaller than the fourfold magnetocrystalline anisotropy (*15*). The uniform vertical orientation of the remanent M is realized even when the axis of the stripe is exactly orthogonal to the easy M direction (Fig. 2C). We conclude that E_m stored in this perpendicular configuration is not enough to demagnetize the stripe, either by domain formation or by rotation of M into equivalent in-plane easy directions, although H_{rev} can be as small as 10 Oe.

The results in Figs. 1 and 2 show that boundaries have a negligible effect on the state of an in-plane magnetized atomically thin film: Domains are not formed, and the easy M axis is not influenced by shape anisotropies. This result is (apparently) in striking contrast with the observation of domains and shape anisotropy reported previously (*4–8, 10, 11*) on patterned films. We propose the following explanation for the contrasting results: Consider the picture of a magnetized body originally put forward by Maxwell (*1*). Accordingly, E_m stored in a uniformly magnetized body with spatial dimension D is formally similar to the Coulomb energy of charged particles distributed on the surface of the body, where the surface charge density is the component of M normal to the boundary. Because the square of the total charge is proportional to $(L^{D-1})^2$ (where L is the linear size of the body) and the Coulomb potential scales with L^{-1}, E_m scales with L^{2D-3}. Domain formation minimizes this energy (*24*). The wall energy E_w acts against the formation of domains (*24*) ($E_w \propto L^{D-1}$). E_m also introduces magnetic anisotropies originating from the actual geometry of the boundaries. In this respect, E_m competes with the magnetocrystalline anisotropy E_a ($\propto L^D$) (*9*) for determining the actual direction of M. Taking into account the scaling dimensions of the various energies, we arrive at the following results in the limit $D = 2$ (which we believe is the one realized by atomically thin films):

1) $E_m^{D=2}$ scales exactly as $E_w^{D=2}$. Thus, reducing the size of the magnetic element does not change the energy balance: There is no need for domains to appear when L is reduced if they were not present for large L, in agreement with the results of Fig. 1. This scaling result is supported by the explicit calculation of the so-called "demagnetizing factor" of in-plane magnetized ultraflat discs (*1*), ultraflat ellipsoids (*2*), and stripes (*23*). At first glance, perpendicularly magnetized continuous films and dots, which contain domains (*3, 5, 25, 26*), seem to represent an exception to our dimensional analysis. However, the origin of perpendicular domains, which appear also for $L \rightarrow \infty$, is the short-range part of the dipolar interaction (*25*) and not the magnetic charge exerted by the boundary. Thus, they must be an exception to our dimensional analysis. Our results on the spatially resolved M of perpendicularly magnetized Fe dots on Cu(100) (see Fig. 3A and compare with Fig. 1E for Co) show the occurrence of stripes within the dots, independent of the dot size.

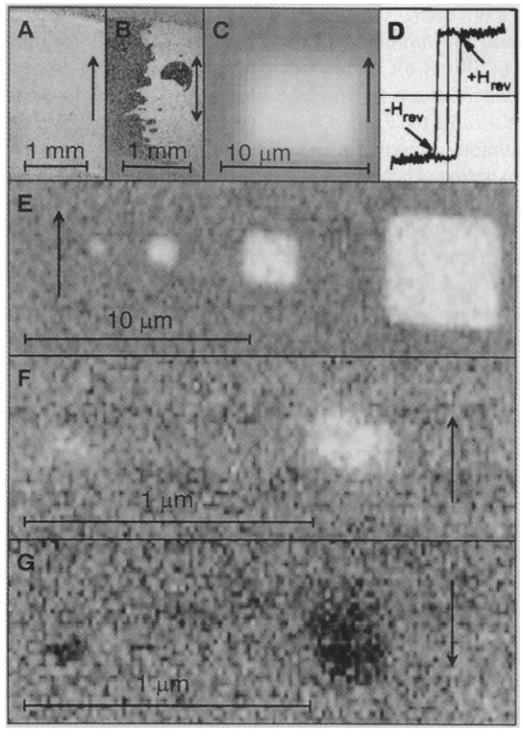

Fig. 1. SEMPA and SKEM images of Co particles with various lateral sizes. The magnetization is measured in the remanent state, that is, after a magnetic field was applied to saturate the sample and subsequently switched off. The gray scale range is taken to be proportional to the spin polarization of the emitted electrons (SEMPA) or to the Kerr asymmetry (SKEM), with gray corresponding to zero spin polarization. The arrows indicate the magnetization direction, which is parallel to a [110] in-plane axis. (**A** and **B**) The surface of an extended Co film (δ = 4.5 AL, H_{rev} = 44 Oe) collected in remanence (A) and after applying a field amounting to $0.995 \cdot (-H_{rev})$ (B). The edge of the Cu substrate is visible at the top and bottom. (**C**) SKEM image of a 9-μm Co dot, 6 AL thick. (**D**) Hysteresis loop collected in the center of the dot in (C) (H_{rev} = 9.5 Oe). (**E**) SEMPA image showing square dots with a size ranging from 0.5 to 4.5 μm and 10 AL thick ($H_{rev} \approx$ 100 Oe). (**F**) SEMPA images of dots with diameters of 130 nm (δ = 2 AL) and 300 nm (δ = 2.5 AL). (**G**) The same dots, after applying a field (340 Oe) larger than $H_{rev} \approx$ 140 Oe, have switched M direction and emit negatively polarized electrons (dark). The image of the 130-nm dot in (F) and (G) consists of ~20 pixels. All of them give the same spin polarization value within experimental uncertainty, so that it is unlikely that an undetected fine structure exists within the dot.

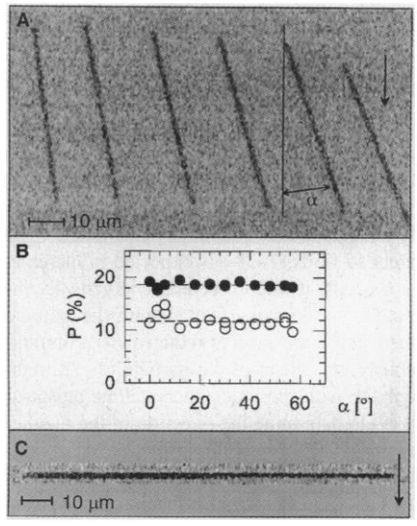

Fig. 2. 2D magnetic stripes. The horizontal in-plane component of M was zero at remanence, within experimental uncertainty. In the thickness and angle range explored in this work, we never detected a nonzero horizontal component at remanence. (**A**) SEMPA image showing a set of Co stripes (23 AL thick) with a variable angle α with respect to the vertical easy direction; M was measured in the remanent state. (**B**) The electron spin polarization measured in the remanent state along the vertical easy axis is plotted as a function of α for two sets of stripes, 40 μm by 0.5 μm, with δ = 3 AL (open circles) and δ = 6 AL (filled circles). H_{rev} varied between ~20 and ~70 Oe. (**C**) SEMPA image of a Co stripe, 122 μm by 1.9 μm (δ = 10 AL), uniformly magnetized perpendicularly to its long axis (black corresponds to a spin polarization of –22%); H_{rev} = 145 Oe.

2) Because $E_a^{D=2}/E_m^{D=2} \propto L$, we expect shape anisotropies to play a role only when L reaches atomic lengths [see also the numerical calculations of (*23*)]. Thus, as long as δ is in the monolayer range, we do not expect shape anisotropies to compete efficiently against magnetocrystalline anisotropies, which are particularly strong in ultrathin films (*9, 15*), in agreement with Fig. 2.

What happens when the particle acquires a finite thickness? In this case, we expect a crossover to $D = 3$, and boundaries should become more effective in demagnetizing the particle, either by introducing domains or by shape anisotropies competing with E_a (or by both effects). As the sample thickness in (*4–8, 10–12*) was several tens of nanometers, this crossover might just be the origin of the observed demagnetizing effects. As shown in Fig. 3B, a "thick" (17 AL) stripe is indeed able to sustain a stable domain with opposite magnetization.

We now address the question of the mutual interaction in an ensemble of 2D particles. Suppose dots are packed within distances comparable to their size L. Each dot acts on neighbors with a field H_m on the order of $M \cdot \delta/L$. Dots act as independent particles if $H_m < H_{rev}$. In $D = 3$ ($\delta \approx L$), H_m is on the order of M (typically 10^3 Oe) independent of the size of the particles. In other words, depending on the balance between H_m and H_{rev}, we expect the mutual interaction of an ensemble of 3D dots to be strong and thus important in determining both the magnetic state of each single dot and their function. In 3D particles, the mutual interaction might have a large influence, for example, on the domain pattern achieved in a matrix (*5, 8*).

We expect 2D particles to behave differently: $H_m^{D=2}$ is reduced by a factor δ/L with respect to $H_m^{D=3}$. We have designed an experimental geometry aimed at measuring the minute dipolar field that we expect to emanate from an in-plane magnetized atomically thin particle (Fig. 4). In this experiment, a small Co particle, which serves as a probe, is sandwiched between two larger elliptical particles that act as a source of magnetic dipolar field. The test particle is exposed to a bias field pointing opposite to the M of the sources. This bias field should help switch M of the test particle from "up" to "down" at a field H_{rev}^- and should oppose the reverse switching process at H_{rev}^+. In situations where H_{rev} of the sources is larger than H_{rev} of the probe, it is possible to switch the magnetic state of the probe back and forth, leaving M of the sources constant (Fig. 4). This allows measurement of the asymmetry $(H_{rev}^- - H_{rev}^+)$, which is less than ~2 Oe. Our numerical estimate of the bias field, obtained by calculating the suitable dipolar sums (*23*), gives $H_m \approx 0.6$ Oe for the geometry of Fig. 4. In line with this result, we have achieved for a variety of situations single-dot manipulation without changing the magnetic state of neighboring dots. Note that a coupling field proportional to δ/L introduces an inherent limit $L_c \approx \delta \cdot M/H_{rev}$ to how close particles can come in 2D: If particles are closer than L_c, they cease to be independent. Our expression for L_c shows that its value might be as small as ~δ, provided $H_{rev} \approx M$.

These observations indicate that in-plane magnetized 2D magnetic particles behave quite differently from 3D ones. Magnetic anisotropies are sufficiently strong to sustain ferromagnetic order against Néel thermal fluctuation instability (*27*) for L down to ~100 nm. At this length scale, the boundaries are quite close but do not introduce domains or a measurable shape anisotropy. As a result, small 2D particles have a nearly square hysteresis curve. Further, we have shown that the magnetostatic interaction between particles is negligible in the 2D limit: Their magnetic state can be manipulated at will and independently of the state of the neighbors. The conditions $D = 2$ and in-plane magnetization are quite essential to these observations, in that (i) they minimize the demagnetizing role of dipolar interaction, and (ii) they maximize (*9*) the role of magnetic anisotropies, so essential for the buildup of a well-defined magnetic state. In light of these results, it might be plausible to speculate that 2D particles maintain these favorable characteristics even in the nanometer range, thus providing well-defined elements for nanorecording.

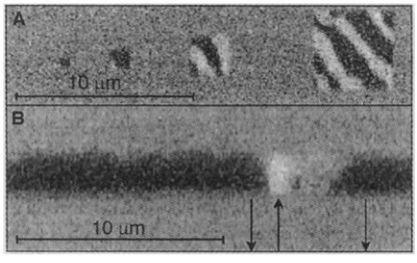

Fig. 3. (**A**) SEMPA image showing ferromagnetic dots of face-centered cubic (fcc) Fe on Cu(100) (δ ≈ 3 AL). The Fe films were deposited at room temperature. The [100] direction lies horizontally. In contrast to Co films, fcc Fe is magnetized perpendicularly to the surface, and its Curie temperature in this thickness range is just above room temperature. Both the continuous film and the dots show the same magnetic structure, consisting of stripe domains oriented along a [110] direction. Only the component of the M perpendicular to the surface is reported; the in-plane component was zero within experimental accuracy. (**B**) SEMPA image of a section of a Co stripe, 122 μm by 1.9 μm (17 AL thick), exposed to 82.5% of H_{rev} = 123 Oe. A white 180° domain is stabilized within the stripe by this procedure. In thinner stripes, exposure to fields as large as 99% of H_{rev} did not produce domains of opposite magnetization.

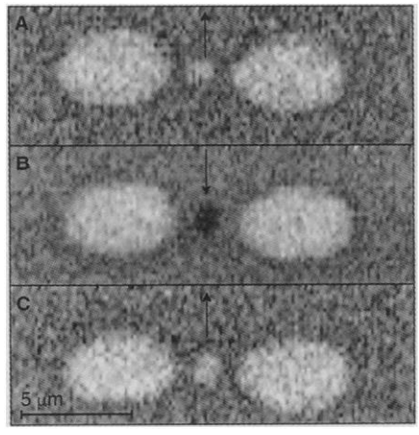

Fig. 4. (**A**) SEMPA image showing a small Co element ($H_{rev} \approx$ 33 Oe) sandwiched between two elliptical particles (H_{rev} = 40 and 36 Oe, δ = 4 AL). Before the image was taken, all of the particles were magnetized "up" by a large positive magnetic field and then exposed to a negative magnetic field of –31 Oe. This negative field did not switch the state of the particles. (**B**) A magnetic field $H_{rev}^- = -33$ Oe has reversed M of the smaller Co dot, which now appears dark in the image. (**C**) A magnetic field $H_{rev}^+ = 33$ Oe has switched M of the smaller Co dot in the positive direction.

References and Notes

1. J. C. Maxwell, *A Treatise on Electricity and Magnetism* (Dover, New York, ed. 3, 1954), vol. 2.
2. E. C. Stoner, *Philos. Mag.* **36**, 803 (1945).
3. R. Allenspach, *J. Magn. Magn. Mater.* **29**, 160 (1994).
4. E. Gu *et al.*, *Phys. Rev. Lett.* **78**, 1158 (1997).
5. M. Hehn *et al.*, *Science* **272**, 1782 (1996).
6. U. Ebels *et al.*, *J. Appl. Phys.* **81**, 4724 (1997).
7. C. Beeli, B. Doudin, J.-Ph. Ansermet, P. A. Stadelmann, *Ultramicroscopy* **67**, 143 (1997).
8. M. S. Wei and S. Y. Chou, *J. Appl. Phys.* **76**, 6679 (1994).
9. R. Q. Wu, L. J. Chen, A. Shick, A. J. Freeman, *J. Magn. Magn. Mater.* **177–181**, 1216 (1998) and references therein.
10. D. D. Awschalom and D. P. DiVincenzo, *Phys. Today* **48**, 43 (1995) and references therein.
11. A. D. Kent, S. von Molnar, S. Gider, D. D. Awschalom, *J. Appl. Phys.* **76**, 6656 (1994).
12. J. F. Smyth *et al.*, *ibid.* **69**, 5262 (1991).
13. M. Lederman, S. Schultz, M. Ozaki, *Phys. Rev. Lett.* **73**, 1986 (1994).
14. W. Wernsdorfer *et al.*, *Phys. Rev. B* **55**, 11552 (1997).
15. P. Krams *et al.*, *Phys. Rev. Lett.* **69**, 3674 (1992); P. Krams *et al.*, *J. Magn. Magn. Mater.* **121**, 483 (1993).
16. U. Ramsperger *et al.*, *Phys. Rev. B* **53**, 8001 (1996).
17. Z. Qiu, J. Pearson, S. D. Bader, *ibid.* **46**, 8659 (1992).
18. H. P. Oepen, *J. Magn. Magn. Mater.* **93**, 116 (1991).
19. W. Dürr, D. Kerkmann, D. Pescia, *Int. J. Mod. Phys. B* **4**, 410 (1990).
20. A. Vaterlaus *et al.*, *Rev. Sci. Instrum.* **68**, 2800 (1997).
21. K. Koike, H. Matsuyama, K. Hayakawa, *Scanning Microsc.* (suppl. 1), 241 (1987).
22. M. R. Scheinfein *et al.*, *Rev. Sci. Instrum.* **61**, 2501 (1990).
23. P. Politi and M. G. Pini, *Eur. Phys. J. B* **2**, 475 (1998).
24. C. Kittel, *Phys. Rev.* **70**, 965 (1946).
25. Y. Yafet and E. M. Gyorgy, *Phys. Rev. B* **38**, 9145 (1988).
26. R. Czech and J. Villain, *J. Phys. Condens. Matter* **1**, 619 (1989).
27. L. Néel, *Rev. Mod. Phys.* **25**, 293 (1953).

28. Supported by the Swiss National Science Foundation and by ETH Zürich through a special grant. We thank the team of Y. Mamaev (St. Petersburg Technical University) for providing the main parts of the Mott detector for the SEMPA experiment and the staff of the Paul Scherrer Institute for technical support.

9 July 1998; accepted 4 September 1998